Highlights

- Aged female PGRN-KO mice show severe low bone mass compared to WT mice.
- PGRN inhibits TNF-α-induced osteoclastogenesis from PGRN-KO mouse spleen cells.
- PGRN promotes osteoblastic differentiation by down-regulating ERK1/2 pathway.

Title

Progranulin plays crucial roles in preserving bone mass by inhibiting TNF-α-induced osteoclastogenesis and promoting osteoblastic differentiation in mice

Author names

Takaaki Noguchi, M.D. [a], Kosuke Ebina, M.D., Ph.D. [a]*, Makoto Hirao, M.D., Ph.D. [a], Ryota Kawase, M.D., Ph.D. [b], Tohru Ohama, M.D., Ph.D. [b c], Shizuya Yamashita, M.D., Ph.D. [b d], Tokimitsu Morimoto, M.D. [a], Kota Koizumi, M.D. [a], Kazuma Kitaguchi, M.D. [a], Hozo Matsuoka, M.D. [a], Shoichi Kaneshiro, M.D., Ph.D. [e], and Hideki Yoshikawa, M.D., Ph.D. [a]

Affiliations

[a] Department of Orthopaedic Surgery, Osaka University, Graduate School of Medicine, 2-2 Yamadaoka, Suita, Osaka 565-0871, Japan.

[b] Department of Cardiovascular Medicine, Osaka University, Graduate School of Medicine, 2-2 Yamadaoka, Suita, Osaka 565-0871, Japan.

[c] Department of Dental Anesthesiology, Osaka University, Graduate School of Medicine, 2-2 Yamadaoka, Suita, Osaka 565-0871, Japan.

[d] Department of Community Medicine, Osaka University, Graduate School of Medicine, 2-2 Yamadaoka, Suita, Osaka 565-0871, Japan.

[e] Department of Orthopaedic Surgery, Japan Community Health Care Organization, Osaka Hospital, 4-2-78 Fukushima ward, Osaka 586-8521, Japan.

***Corresponding author:**

Phone: +81 6 6879 3552; FAX: +81 6 6879 3559

E-mail address: k-ebina@umin.ac.jp (K. Ebina)

Abstract

A close correlation between atherosclerosis, inflammation, and osteoporosis has been recognized, although the precise mechanism remains unclear. The growth factor progranulin (PGRN) is expressed in various cells such as macrophages, leukocytes, and chondrocytes. PGRN plays critical roles in a variety of diseases, such as

atherosclerosis and arthritis by inhibiting Tumor Necrosis Factor-α (TNF-α) signaling. The purpose of this study was to investigate the effect of PGRN on bone metabolism. Forty-eight-week old female homozygous PGRN knockout mice (PGRN-KO) (n=8) demonstrated severe low bone mass in the distal femur compared to age- and sex-matched wild type C57BL/6J mice (WT) (n=8) [BV/TV (%): 5.8 vs. 16.6; p<0.001, trabecular number (1/mm): 1.6 vs. 3.8; p<0.001]. *In vitro*, PGRN inhibited TNF-α-induced osteoclastogenesis from spleen cells of PGRN-KO mice (vehicle→5→50 ng/ml PGRN: 172.3→138.0→132.0 number of osteoclasts per six fields; vehicle vs. 50 ng/ml, p<0.05). Moreover, PGRN significantly promoted ALP activity (vehicle→5→50 ng/ml PGRN: 28.1→36.5→51.7 ALP/protein units/μg protein; vehicle vs. 50 ng/ml, p<0.05), osteoblast-related mRNA (ALP, osteocalcin) expression in a dose-dependent manner and up-regulated osteoblastic differentiation by down-regulating phosphorylation of ERK1/2 in mouse calvarial cells. In conclusion, PGRN may be a promising treatment target for both atherosclerosis and inflammation-related osteoporosis.

Keywords

Progranulin, osteoclast, osteoblast, TNF-α, bone metabolism, ERK1/2.

1. Introduction

Recent reports have demonstrated a close correlation between atherosclerosis, inflammation, and osteoporosis [1-7], and the existence of common factors has been assumed. TNF-α is strongly associated with both atherosclerosis and arthritis [8, 9], and also promotes osteoclastogenesis and inhibits osteoblastogenesis [10, 11]. PGRN is a 593 amino acid autocrine growth factor, which shows protective effects against Alzheimer's disease and wound healing [12, 13]. Recent reports demonstrated that PGRN inhibits TNF-α signaling and plays critical roles in the pathology of atherosclerosis and arthritis [14-16]. Conversely, PGRN enhances endochondral ossification during development and also acts as a critical mediator of the bone healing process modulating BMP-2 and TNF-α signaling [17]. However, another recent report demonstrated that serum PGRN levels were substantially higher in ovariectomized mice than in sham control mice and PGRN strongly induced osteoclastogenesis in the presence of Receptor Activator of Nuclear factor Kappa-B Ligand (RANKL) [18]. Collectively, the physiological role of PGRN in bone metabolism seems controversial. In this study, we demonstrate a difference in bone mass of the distal femurs between homozygous PGRN-KO mice and WT mice and investigate the direct effect of PGRN on TNF-α-induced osteoclastogenesis and osteoblastic differentiation *in vitro*.

2. Materials and methods

2.1. Animals

Homozygous PGRN-KO mice with a C57BL/6J background were obtained from Riken BioResource Center (Tsukuba, Japan) [19], and WT mice with a C57BL/6J background were obtained from Charles River Laboratories (Osaka, Japan). Experiments were performed using age- and sex-matched PGRN-KO mice and WT mice, which were fed with normal chow and water from birth to 48 weeks in a temperature- and humidity-controlled facility with a 12 hour light/dark cycle. Mice were anaesthetized with an intraperitoneal injection of 5.0 mg/kg butorphanol, 4.0 mg/kg midazolam, and 0.3 mg/kg medetomidine and then sacrificed [20]. All experimental protocols were approved by the Ethics Review Committee for animal Experimentation of Osaka University, Graduate School of Medicine.

2.2 Micro-CT

The distal femurs of mice (500 μm above the growth plate) were evaluated by micro-computed tomography (micro-CT) (Rigaku Mechatronics, Tokyo, Japan) and the results were analyzed using Tri/3D Bon software (Ratoc System Engineering Co., Ltd.,

Tokyo, Japan) for various parameters including total volume (TV), bone volume (BV), BV/TV, trabecular thickness (TbTh), trabecular number (TbN), trabecular space (TbS), cortical volume (Cv), all volume (Av), Cv/Av and mean cortical bone thickness.

2.3. Histology

After micro-CT scans, specimens were fixed in 10% neutral-buffered and decalcified for embedding. Histological sections were stained with tartrate resistant acid phosphatase (TRAP) following the manufacturer's protocol (Cosmo bio, Tokyo, Japan). The area of TRAP-positive osteoclasts per unit trabecular surface was counted as previously described [21].

2.4. Immunohistochemistry

Sections were incubated with anti-osteocalcin antibody (Takara bio, Shiga, Japan) according to the manufacturer's protocol. The next day, the sections were incubated for 30 minutes with secondary antibody (Vectastain Elite ABC kit Rabbit IgG: Vector Laboratories, Inc., San Diego, CA, USA) and stained with 3, 3'-Diaminobenzidine tetrahydrochloride (DAB) (Dako, Tokyo, Japan).

2.5. Serum assay

Serum concentration of osteocalcin (Takara Bio), CTX-1 (CUSABIO, Hubei, China), and TNF-α (R&D Systems, Minneapolis, MN, USA) were measured by ELISA kit according to the manufacturer's protocol.

2.6. Cell culture

Mouse spleen-derived cells and mouse bone marrow-derived cells flushed from the femur and tibia were cultured in α-minimum essential medium (α-MEM) containing 10% fetal bovine serum (FBS) (Equitech-Bio, Kerrville, TX, USA) and 1% penicillin and streptomycin overnight at 37℃ in a humidified atmosphere of 5% CO_2. Adherent cells were seeded at 1×10^6 cells per well in a 12-well plate and then stimulated with 10 ng/ml M-CSF (R&D Systems) and 50 ng/ml RANKL (R&D Systems) as previously described [22]. The following day, cells were stimulated with TNF-α (R&D Systems) (vehicle, 1, 5 or 10 ng/ml) and mouse recombinant PGRN protein (R&D Systems) (vehicle, 5 or 50 ng/ml) simultaneously for 5 days in a 48-well plate.

MC3T3-E1 cells were purchased from Riken Cell Bank (Tsukuba, Japan) and murine primary osteoblasts were isolated from the calvaria of three-day old C57BL/6J mice. Cells were seeded at 1×10^5 cells per well in a 12-well plate or 5×10^4 cells per well in a 24-well plate, and treated with mouse recombinant PGRN protein (vehicle, 5, 50 or 100 ng/ml) for 5 days. Media were changed to osteoblast differentiation medium containing

50 μg/ml ascorbic acid (Sigma-Aldrich, St. Louis, MO, USA) and 10 mM β-glycerophosphate (Calbiochem, San Diego, CA, USA) after the cells reached 60-70% confluence.

2.7. TRAP staining

Cells were washed once with PBS and fixed with 10% formalin. TRAP staining was performed using a TRAP staining kit (Cosmo Bio) according to the manufacturer's protocol. The total number of TRAP-positive cells with three or more nuclei was counted in six fields [23].

2.8. Alkaline phosphatase (ALP) staining, ALP activity assay, and Alizarin red staining

Osteoblastic cells were treated with PGRN (vehicle, 5 or 50 ng/ml) and incubated for 5 days. For ALP staining, cells were washed twice with PBS after fixation with 10% formalin and incubated with ALP substrate solution, 0.1 mg/ml naphthol AS-MX (Sigma-Aldrich), and 0.6 mg/ml fast violet B salt (Sigma-Aldrich) in 0.1 M Tris-HCl for 30 minutes. For the ALP activity assay, cells were washed twice with PBS and lysed with Mammalian Protein Extraction Reagent (Pierce, Rockford, IL, USA), and ALP activity was measured using a Lab Assay ALP activity kit (Wako Pure Chemical Industries, Ltd., Osaka, Japan) according to the manufacturer's protocol. ALP protein was quantified

using the Bicinchoninic Acid Protein Assay Kit (Pierce). For Alizarin red staining, cells were washed once with distilled water (DW) after fixation with 10% formalin and stained with alizarin red solution (PG Research Inc., Tokyo, Japan) according to the manufacturer's protocol. Absorbance of the released alizarin red was measured at 415 nm with a microplate reader [24].

2.9. Extraction of RNA from bone tissue and cells and first-strand cDNA synthesis

RNA was extracted from the radial bone of PGRN-KO and WT mice according to the QIAzol standard protocol (Qiagen, Düsseldorf, Germany). RNA was extracted from cells in 12-well plate using a RNAeasy Mini Kit (Qiagen). First-strand cDNA was reverse-transcribed from total RNA (1 μg) using the SuperScriptⅢ First-Strand Synthesis system (Life Technologies, Tokyo, Japan).

2.10. Quantitative real-time PCR analysis

Real-time PCR was performed using a Step One Plus Real-Time PCR System (Life Technologies) and Fast SYBR Green Master Mix (Life Technologies), in which each cDNA sample was evaluated and expression values were normalized to GAPDH. PCR primers (forward and reverse, respectively) were as follows: *GAPDH*, 5'-AGGTCGGTGTGAACGGATTTG-3' and 5'-TGTAGACCATGTAGTTGAGGTCA-3';

154 *ALP*, 5’-AATCGGAACAACCTGACTGACC-3’ and

155 5’-TCCTTCCACCAGCAAGAAGAA-3’; *Osteocalcin*, 5’-CTCACTCTGCTGGCCCTG-3’

156 and 5’-CCGTAGATGCGTTTGTAGGC-3’; *TNF-α,*

157 5’-GGACAGTGACCTGGACTGTGG-3’ and 5’-AGTGAATTCGGAAAGCCCATT-3’; *IL-6,*

158 5’-ACAACCACGGCCTTCCCTACTT-3’ and 5’-CACGATTTCCCAGAGAACATGTG-3’.

159 2.11. Western blotting

160 Cells from mouse calvaria were cultured in 12-well plates and homogenized with 100 μl

161 of RIPA buffer (Pierce), and complete cell lysis was obtained using a sonicator for 7.5

162 minutes. The lysates were centrifuged at 12,000 rpm for 5 minutes at 4℃ and the

163 supernatants were used for electrophoresis after a protein assay using a BCA assay kit

164 (Pierce) [25]. Western blotting was performed using the following antibodies purchased

165 from Cell Signaling Technology (Danvers, MA, USA): phosphate anti-Akt antibody

166 (Ser473) (1:2000), anti-Akt antibody (pan) (1:1000), phosphate anti-ERK1/2 antibody

167 (Thr202/Tyr204) (1:2000), anti-ERK1/2 antibody (p44/42) (1:1000), phosphate anti-p38

168 antibody (Thr180/Tyr182) (1:1000), anti-p38 antibody (1:1000), phosphate

169 anti-SAPK/JNK antibody (Thr183/Tyr185) (1:1000), anti-SAPK/JNK antibody (1:1000),

170 phosphate anti-β-Catenin antibody (Ser675) (1:1000), anti-β-Catenin antibody (1:1000),

171 and anti-β-actin antibody (1:2000).

2.12. Statistical analysis

All data were expressed as mean ± standard deviation (SD). Differences between the groups were assessed by a Mann-Whitney U-test. A probability value of <0.05 was considered to indicate statistical significance.

3. Results

3.1. Decreased trabecular bone mass in homozygous PGRN-KO mice

Trabecular and cortical bone in the distal femur were assessed by micro-CT (Fig. 1A). The values of BV/TV and TbN in PGRN-KO mice were significantly decreased compared to WT mice, while TbS in PGRN-KO mice was significantly increased compared to WT mice (Fig. 1B). No significant differences were observed in the cortical bone parameters (Cv/Av, cortical bone thickness) between the groups (Fig. 1C). TRAP staining of the distal femur demonstrated a significantly larger number of osteoclasts in PGRN-KO mice compared to WT mice (Fig. 2A, B). On the other hand, immunostaining of osteocalcin revealed that the number of osteocalcin–positive cells was smaller in PGRN-KO mice compared to WT mice (Fig. 2C). Gene expression levels of TNF-α and IL-6 in bone tissue were higher in PGRN-KO mice compared to WT mice as evaluated

189 by real-time PCR (Fig. 2D). ELISA of serum bone turnover markers revealed that
190 osteocalcin levels were significantly lower and TNF-α levels were significantly higher in
191 PGRN-KO mice compared to WT mice (Fig. 2E).

192 3.2. Effects of PGRN on osteoclastogenesis

193 The effect of PGRN on osteoclastogenesis *in vitro* was evaluated. Osteoclast
194 differentiation was induced by TNF-α (vehicle, 1, 5 or 10 ng/ml) using spleen cells of
195 PGRN-KO and WT mice. The number of osteoclasts did not change in WT mice, while
196 they were significantly increased in PGRN-KO mice in a dose-dependent manner (Fig.
197 3A, B). After inducing osteoclast differentiation by adding 10 ng/ml TNF-α to cells of
198 PGRN-KO mice, treatment with PGRN recombinant protein (vehicle, 5, or 50 ng/ml)
199 significantly decreased the number of TRAP-positive cells in a dose-dependent manner
200 (Fig. 3C, D).

201 3.3. Effects of PGRN on osteoblasts

202 PGRN significantly promoted ALP activity of MC3T3-E1 cells (Fig. 4A) and WT mouse
203 calvarial cells (Fig. 4B). In addition, PGRN significantly promoted osteoblast-related
204 mRNA (ALP, osteocalcin) expression in a dose-dependent manner (Fig. 4C).
205 Consequently, PGRN promoted mineralization of MC3T3-E1 cells as evaluated by

Alizarin red stain (Fig. 4D). Western blotting revealed that PGRN down-regulated the phosphorylation of ERK1/2 and p38 in a dose dependent manner (Fig. 4E).

4. Discussion

We have previously demonstrated that PGRN plays important roles in atherogenesis by modulation of local and systemic inflammation [26]. Pro-inflammatory cytokines such as TNF-α enhance osteoclastogenesis partially by inducing RANKL from various cells [10, 11]. Previous reports showed that PGRN binds directly to the Tumor Necrosis Factor receptor (TNFR) and disrupts TNF-α signaling [14, 15, 17]. Therefore, we hypothesized that PGRN may play an important role in bone metabolism, especially in inflammatory conditions. In this study, we have demonstrated for the first time that physiological levels of PGRN (35-70 ng/ml) [27] inhibits TNF-α-induced osteoclastogenesis and also promotes osteoblastogenesis. Furthermore, aged homozygous PGRN-KO mice showed an increased number of osteoclasts and severe trabecular bone loss in the distal femur compared to WT mice.

Concerning osteoclastogenesis, a recent report demonstrated that PGRN-KO mice showed a higher number of osteoclasts and lower bone mineral density (BMD) in

223 vertebra compared to WT mice, but no *in vitro* data were shown [28]. However, another
224 recent report showed hyper-physiological levels of PRGN (500 ng/ml) promotes
225 multinucleated osteoclast formation and bone resorption from mouse bone marrow cells
226 when stimulated with M-CSF (30 ng/ml) and RANKL (100 ng/ml) [18]. In this study, we
227 demonstrate that physiological levels of PGRN inhibited osteoclastogenesis of
228 PGRN-KO mouse spleen cells induced by TNF-α. However, even hyper-physiological
229 levels of PRGN (200 ng/ml) showed no significant effects on osteoclastogenesis of WT
230 mice spleen cells induced by TNF-α or of WT mouse bone marrow cells induced by
231 M-CSF and RANKL (data not shown). Taken together, a depletion of physiological
232 levels of PGRN may lead to elevated serum and local TNF-α levels, which may promote
233 osteoclastogenesis and consequent bone loss in aged mice.

234 Concerning osteoblastogenesis, a previous report demonstrated that PGRN was
235 required for BMP-2-induced osteoblastogenesis *in vitro*, although they only showed the
236 effect of recombinant PGRN protein on Runx2 gene expression of C2C12 cells [17]. In
237 this study, PGRN-KO mice showed significantly lower levels of serum osteocalcin
238 compared to WT mice. In addition, physiological levels of PGRN down-regulated the
239 phosphorylation of ERK1/2 which signaling inhibition leads to osteoblast differentiation
240 [29], and consequently promoted ALP activity, osteoblast-related gene expression

241 (ALP, osteocalcin), and mineralization of mouse calvarial cells and MC3T3-E1 cells.
242 These results clearly demonstrate that physiological levels of PGRN are effective in
243 promoting osteoblastogenesis.

244 In conclusion, PGRN may be one of the crucial factors to maintain bone mass,
245 especially in aged mice, where it may play interactive roles in both inhibiting
246 TNF-α-induced osteoclastogenesis and promoting osteoblastogenesis by
247 down-regulating phosphorylation of ERK1/2.

248

249 **Acknowledgments**

250 We are grateful to M. Shinkawa and A. Tada for excellent technical assistance. We
251 thank all the members of Dr. Yoshikawa's and Dr. Yamashita's laboratories for the
252 helpful discussion and comments.

253

254 **References**

255 [1] J.R. Shaffer, C.M. Kammerer, D.L. Rainwater, D.H. O'Leary, J.M. Bruder, R.L. Bauer,
256 B.D. Mitchell, Decreased bone mineral density is correlated with increased subclinical

257 atherosclerosis in older, but not younger, Mexican American women and men: the San
258 Antonio Family Osteoporosis Study, Calcified tissue international, 81 (2007) 430-441.

259 [2] K. Ebina, A. Fukuhara, W. Ando, M. Hirao, T. Koga, K. Oshima, M. Matsuda, K. Maeda, T.
260 Nakamura, T. Ochi, I. Shimomura, H. Yoshikawa, J. Hashimoto, Serum adiponectin
261 concentrations correlate with severity of rheumatoid arthritis evaluated by extent of joint
262 destruction, Clinical rheumatology, 28 (2009) 445-451.

263 [3] K. Ebina, K. Oshima, M. Matsuda, A. Fukuhara, K. Maeda, S. Kihara, J. Hashimoto, T.
264 Ochi, N.K. Banda, H. Yoshikawa, I. Shimomura, Adenovirus-mediated gene transfer of
265 adiponectin reduces the severity of collagen-induced arthritis in mice, Biochemical and
266 biophysical research communications, 378 (2009) 186-191.

267 [4] S. Khosla, The bone and beyond: a shift in calcium, Nature medicine, 17 (2011) 430-431.

268 [5] B.I. Freedman, T.C. Register, Effect of race and genetics on vitamin D metabolism, bone
269 and vascular health, Nature reviews. Nephrology, 8 (2012) 459-466.

270 [6] K. Ebina, K. Shi, M. Hirao, S. Kaneshiro, T. Morimoto, K. Koizumi, H. Yoshikawa, J.
271 Hashimoto, Vitamin K2 administration is associated with decreased disease activity in
272 patients with rheumatoid arthritis, Modern rheumatology / the Japan Rheumatism
273 Association, 23 (2013) 1001-1007.

[7] S. Kaneshiro, K. Ebina, K. Shi, C. Higuchi, M. Hirao, M. Okamoto, K. Koizumi, T. Morimoto, H. Yoshikawa, J. Hashimoto, IL-6 negatively regulates osteoblast differentiation through the SHP2/MEK2 and SHP2/Akt2 pathways in vitro, Journal of bone and mineral metabolism, 32 (2014) 378-392.

[8] I.A. Ku, J.B. Imboden, P.Y. Hsue, P. Ganz, Rheumatoid arthritis: model of systemic inflammation driving atherosclerosis, Circulation journal : official journal of the Japanese Circulation Society, 73 (2009) 977-985.

[9] L. Rodriguez-Rodriguez, C. Gonzalez-Juanatey, R. Palomino-Morales, T.R. Vazquez-Rodriguez, J.A. Miranda-Filloy, B. Fernandez-Gutierrez, J. Llorca, J. Martin, M.A. Gonzalez-Gay, TNFA -308 (rs1800629) polymorphism is associated with a higher risk of cardiovascular disease in patients with rheumatoid arthritis, Atherosclerosis, 216 (2011) 125-130.

[10] K. Kobayashi, N. Takahashi, E. Jimi, N. Udagawa, M. Takami, S. Kotake, N. Nakagawa, M. Kinosaki, K. Yamaguchi, N. Shima, H. Yasuda, T. Morinaga, K. Higashio, T.J. Martin, T. Suda, Tumor necrosis factor alpha stimulates osteoclast differentiation by a mechanism independent of the ODF/RANKL-RANK interaction, The Journal of experimental medicine, 191 (2000) 275-286.

291 [11] M.S. Nanes, Tumor necrosis factor-alpha: molecular and cellular mechanisms in skeletal
292 pathology, Gene, 321 (2003) 1-15.

293 [12] Z. He, C.H. Ong, J. Halper, A. Bateman, Progranulin is a mediator of the wound
294 response, Nature medicine, 9 (2003) 225-229.

295 [13] S. Pereson, H. Wils, G. Kleinberger, E. McGowan, M. Vandewoestyne, B. Van Broeck,
296 G. Joris, I. Cuijt, D. Deforce, M. Hutton, C. Van Broeckhoven, S. Kumar-Singh, Progranulin
297 expression correlates with dense-core amyloid plaque burden in Alzheimer disease mouse
298 models, The Journal of pathology, 219 (2009) 173-181.

299 [14] C.J. Liu, Progranulin: a promising therapeutic target for rheumatoid arthritis, FEBS
300 letters, 585 (2011) 3675-3680.

301 [15] W. Tang, Y. Lu, Q.Y. Tian, Y. Zhang, F.J. Guo, G.Y. Liu, N.M. Syed, Y. Lai, E.A. Lin, L.
302 Kong, J. Su, F. Yin, A.H. Ding, A. Zanin-Zhorov, M.L. Dustin, J. Tao, J. Craft, Z. Yin, J.Q.
303 Feng, S.B. Abramson, X.P. Yu, C.J. Liu, The growth factor progranulin binds to TNF
304 receptors and is therapeutic against inflammatory arthritis in mice, Science, 332 (2011)
305 478-484.

306 [16] H.J. Hwang, T.W. Jung, H.C. Hong, H.Y. Choi, J.A. Seo, S.G. Kim, N.H. Kim, K.M. Choi,
307 D.S. Choi, S.H. Baik, H.J. Yoo, Progranulin protects vascular endothelium against

atherosclerotic inflammatory reaction via Akt/eNOS and nuclear factor-kappaB pathways, PloS one, 8 (2013) e76679.

[17] Y.P. Zhao, Q.Y. Tian, S. Frenkel, C.J. Liu, The promotion of bone healing by progranulin, a downstream molecule of BMP-2, through interacting with TNF/TNFR signaling, Biomaterials, 34 (2013) 6412-6421.

[18] J. Oh, J.Y. Kim, H.S. Kim, J.C. Oh, Y.H. Cheon, J. Park, K.H. Yoon, M.S. Lee, B.S. Youn, Progranulin and a five transmembrane domain-containing receptor-like gene are the key components in receptor activator of nuclear factor kappaB (RANK)-dependent formation of multinucleated osteoclasts, The Journal of biological chemistry, 290 (2015) 2042-2052.

[19] Y. Kayasuga, S. Chiba, M. Suzuki, T. Kikusui, T. Matsuwaki, K. Yamanouchi, H. Kotaki, R. Horai, Y. Iwakura, M. Nishihara, Alteration of behavioural phenotype in mice by targeted disruption of the progranulin gene, Behavioural brain research, 185 (2007) 110-118.

[20] S. Kawai, Y. Takagi, S. Kaneko, T. Kurosawa, Effect of three types of mixed anesthetic agents alternate to ketamine in mice, Experimental animals / Japanese Association for Laboratory Animal Science, 60 (2011) 481-487.

[21] Y. He, S.D. Rhodes, S. Chen, X. Wu, J. Yuan, X. Yang, L. Jiang, X. Li, N. Takahashi, M. Xu, K.S. Mohammad, T.A. Guise, F.C. Yang, c-Fms signaling mediates neurofibromatosis Type-1 osteoclast gain-in-functions, PloS one, 7 (2012) e46900.

[22] M. Okamoto, J. Murai, Y. Imai, D. Ikegami, N. Kamiya, S. Kato, Y. Mishina, H. Yoshikawa, N. Tsumaki, Conditional deletion of Bmpr1a in differentiated osteoclasts increases osteoblastic bone formation, increasing volume of remodeling bone in mice, Journal of bone and mineral research : the official journal of the American Society for Bone and Mineral Research, 26 (2011) 2511-2522.

[23] C.T. Ritchlin, S.A. Haas-Smith, P. Li, D.G. Hicks, E.M. Schwarz, Mechanisms of TNF-alpha- and RANKL-mediated osteoclastogenesis and bone resorption in psoriatic arthritis, The Journal of clinical investigation, 111 (2003) 821-831.

[24] T. Miyazaki, S. Miyauchi, A. Tawada, T. Anada, S. Matsuzaka, O. Suzuki, Oversulfated chondroitin sulfate-E binds to BMP-4 and enhances osteoblast differentiation, Journal of cellular physiology, 217 (2008) 769-777.

[25] Y. Imura, H. Yasui, H. Outani, T. Wakamatsu, K. Hamada, T. Nakai, S. Yamada, A. Myoui, N. Araki, T. Ueda, K. Itoh, H. Yoshikawa, N. Naka, Combined targeting of mTOR and

c-MET signaling pathways for effective management of epithelioid sarcoma, Molecular cancer, 13 (2014) 185.

[26] R. Kawase, T. Ohama, A. Matsuyama, T. Matsuwaki, T. Okada, T. Yamashita, M. Yuasa-Kawase, H. Nakaoka, K. Nakatani, M. Inagaki, K. Tsubakio-Yamamoto, D. Masuda, Y. Nakagawa-Toyama, M. Nishida, Y. Ohmoto, M. Nishihara, I. Komuro, S. Yamashita, Deletion of progranulin exacerbates atherosclerosis in ApoE knockout mice, Cardiovascular research, 100 (2013) 125-133.

[27] A. Tanaka, H. Tsukamoto, H. Mitoma, C. Kiyohara, N. Ueda, M. Ayano, S. Ohta, Y. Inoue, Y. Arinobu, H. Niiro, T. Horiuchi, K. Akashi, Serum progranulin levels are elevated in patients with systemic lupus erythematosus, reflecting disease activity, Arthritis research & therapy, 14 (2012) R244.

[28] Y.P. Zhao, Q.Y. Tian, B. Liu, J. Cuellar, B. Richbourgh, T.H. Jia, C.J. Liu, Progranulin knockout accelerates intervertebral disc degeneration in aging mice, Scientific reports, 5 (2015) 9102.

[29] S.J. Kono, Y. Oshima, K. Hoshi, L.F. Bonewald, H. Oda, K. Nakamura, H. Kawaguchi, S. Tanaka, Erk pathways negatively regulate matrix mineralization, Bone, 40 (2007) 68-74.

Figure Legends

Fig. 1. (A) Micro-CT images of the distal femur from forty-eight-week old WT and PGRN-KO mice. (B) Quantitation of trabecular bone parameters (BV/TV, TbN, TbTh and TbS). (C) Quantitation of cortical bone parameters (Cv/Av and Mean cortical bone thickness). Data are the mean ± SD for 8 mice of each group. ***p<0.001 WT vs. PGRN-KO mice.

Fig. 2. (A) TRAP staining in the distal femur of WT and PGRN-KO mice (200×). (B) The number of TRAP-positive cells per unit trabecular surface (200×). ***p<0.001 WT vs. PGRN-KO mice. (C) Immunostaining of osteocalcin in the distal femur of WT and PGRN-KO mice (200×). (D) Gene expression of TNF-α and IL-6 in bone tissue of WT and PGRN-KO mice assessed by real-time PCR. (E) Serum levels of osteocalcin, CTX1 and TNF-α of WT and PGRN-KO mice assessed by ELISA. **p<0.01, *p<0.05 WT vs. PGRN-KO mice. All data are expressed as the mean ± SD.

Fig. 3. (A) (B) Induction of osteoclasts from spleen cells of WT and PGRN-KO mice under TNF-α stimuli assayed by TRAP-staining. *p<0.05 WT vs. PGRN-KO mice,

†p<0.05 vs. vehicle (200×). (C) (D) Induction of osteoclasts from spleen cells of PGRN-KO mice under TNF-α stimuli and treatment with PGRN assayed by TRAP-staining *p<0.05 vs. vehicle (200×). All data are expressed as the mean ± SD.

Fig. 4. (A) ALP activity in MC3T3-E1 cells treated with PGRN. *p<0.05 vs. vehicle. (B) ALP activity in mouse calvarial cells treated with PGRN. *p<0.05 vs. vehicle. (C) ALP and osteocalcin gene expression change in mouse calvarial cells treated with PGRN. *p<0.05 vs. vehicle. (D) Mineralization of MC3T3-E1 cells treated with PGRN assayed by Alizarin red staining. *p<0.05 vs. vehicle. (E) Western blotting analysis of the phosphorylation of osteoblast differentiation-related signals in mouse calvarial cells. All data are expressed as the mean ± SD.

The word count is 3839.

Figure

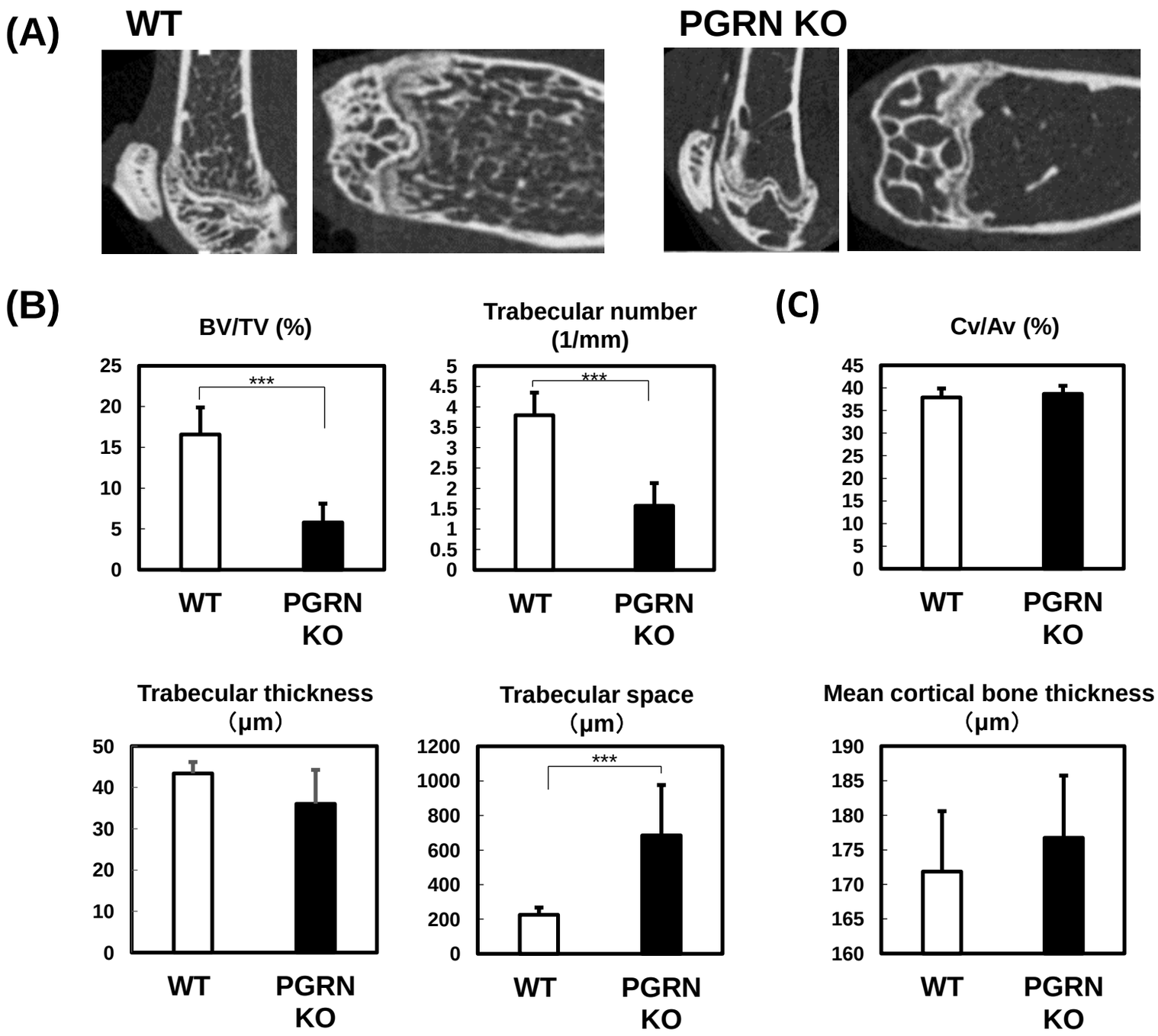
(A)
WT
PGRN KO
(B)
BV/TV (%)
***
25
20
15
10
5
0
WT
PGRN KO
Trabecular number (1/mm)
***
5
4.5
4
3.5
3
2.5
2
1.5
1
0.5
0
WT
PGRN KO
(C)
Cv/Av (%)
45
40
35
30
25
20
15
10
5
0
WT
PGRN KO
Trabecular thickness (μm)
50
40
30
20
10
0
WT
PGRN KO
Trabecular space (μm)
***
1200
1000
800
600
400
200
0
WT
PGRN KO
Mean cortical bone thickness (μm)
190
185
180
175
170
165
160
WT
PGRN KO

(A)

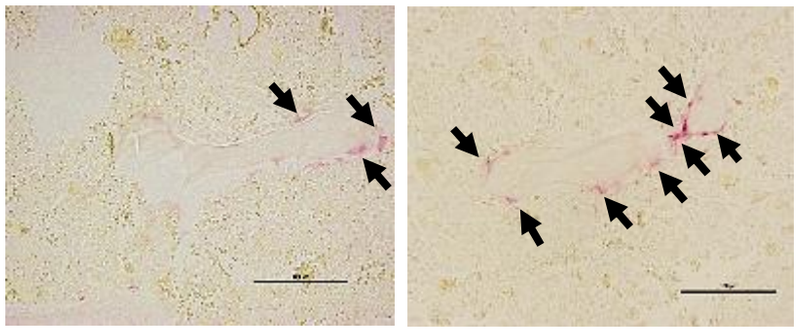

WT PGRN KO

(B)

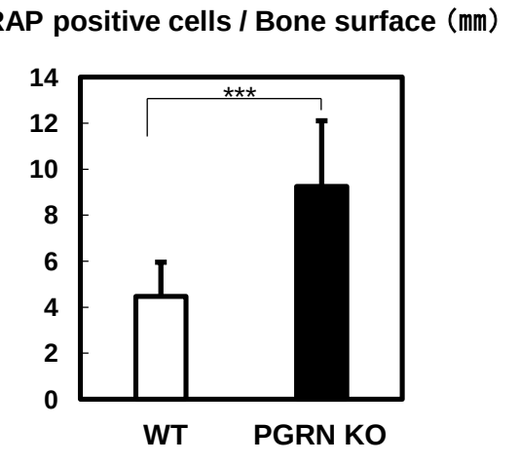

(C)

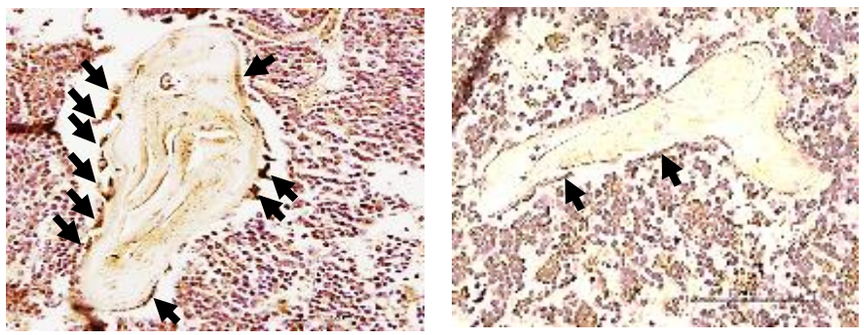

WT PGRN KO

(D)

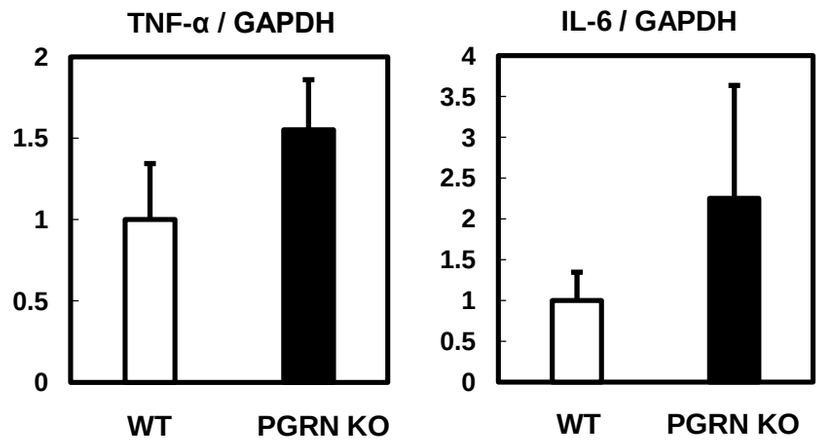

(E)

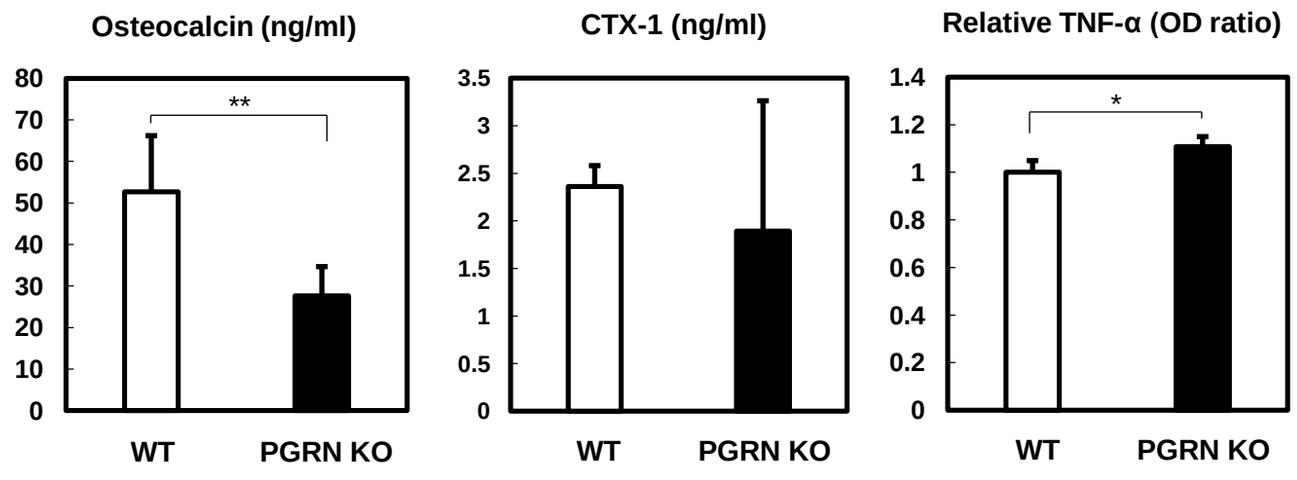

(A)

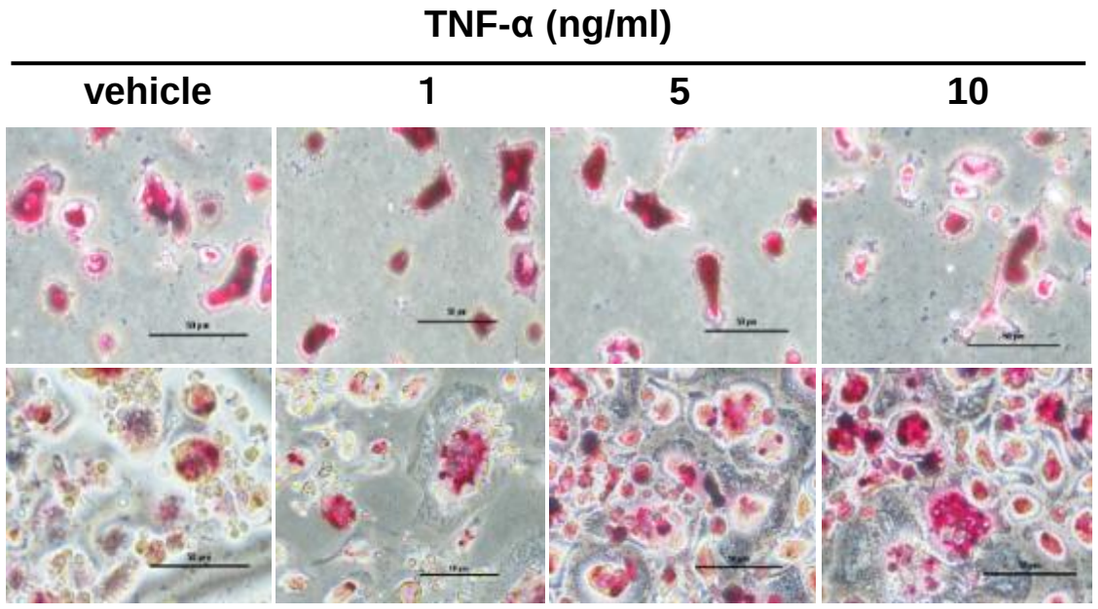
TNF-α (ng/ml)
vehicle
1
5
10
WT
PGRN KO

(B)

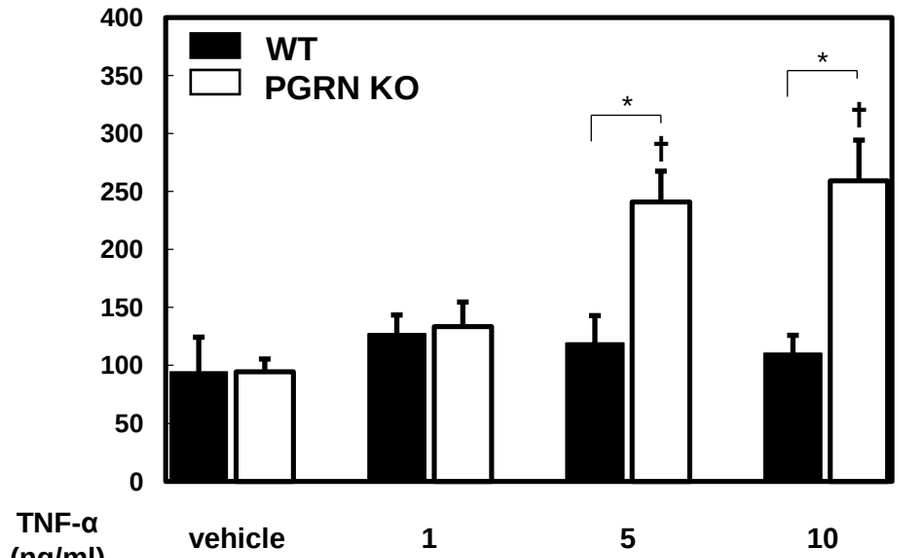
Total Number of TRAP positive cells
400
350
300
250
200
150
100
50
0
WT
PGRN KO
*
†
TNF-α (ng/ml)
vehicle
1
5
10

(C)

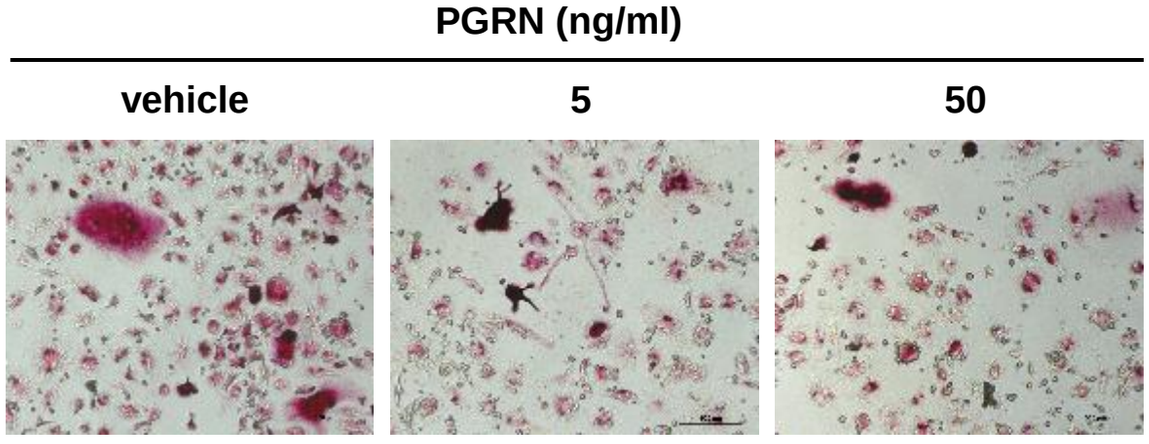
PGRN (ng/ml)
vehicle
5
50
PGRN KO + TNF-α 10ng/ml

(D)

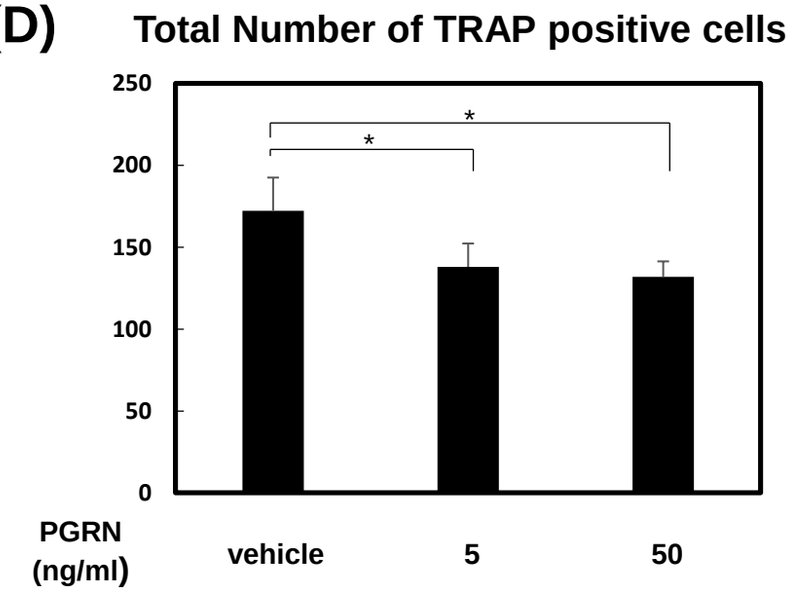
Total Number of TRAP positive cells
250
200
150
100
50
0
*
PGRN (ng/ml)
vehicle
5
50

(A)

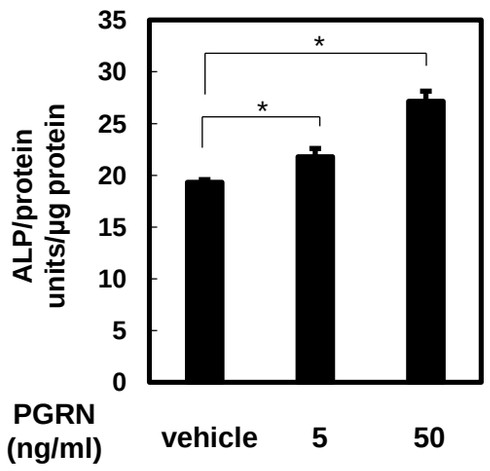
ALP activity
ALP/protein units/μg protein
35
30
25
20
15
10
5
0
*
*
PGRN (ng/ml)
vehicle
5
50

(B)

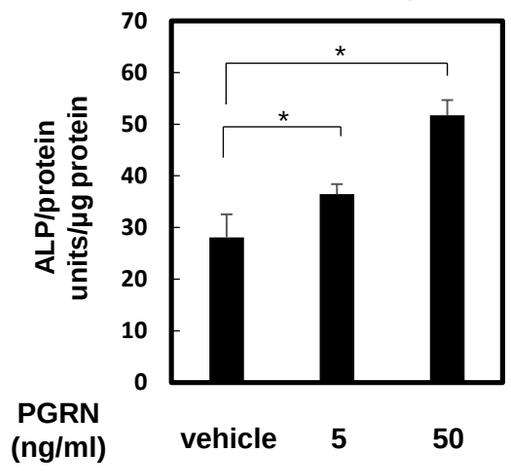
ALP activity
ALP/protein units/μg protein
70
60
50
40
30
20
10
0
*
*
PGRN (ng/ml)
vehicle
5
50

(C)

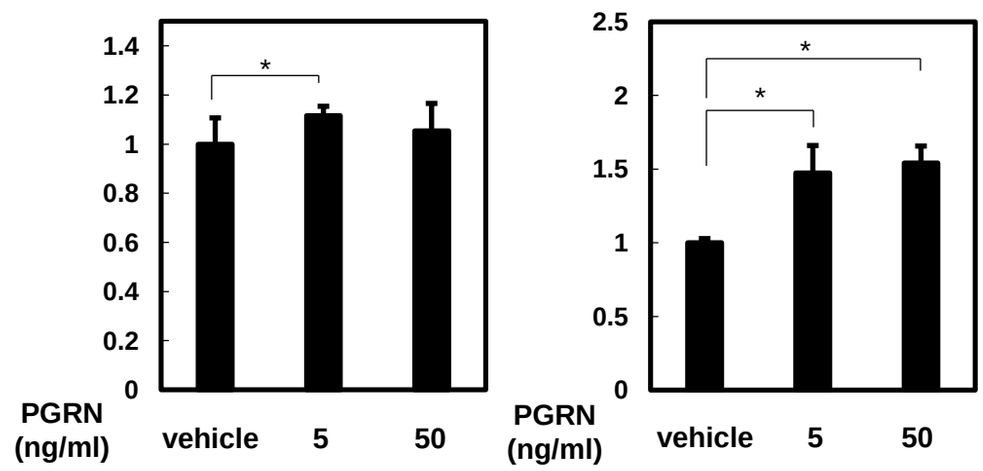
ALP / GAPDH
1.4
1.2
1
0.8
0.6
0.4
0.2
0
*
PGRN (ng/ml)
vehicle
5
50
Osteocalcin / GAPDH
2.5
2
1.5
1
0.5
0
*
*
PGRN (ng/ml)
vehicle
5
50

(D)

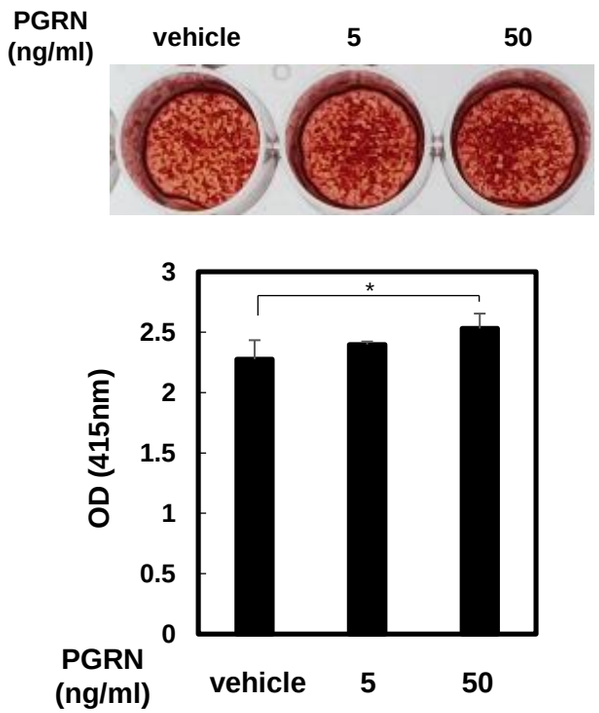
PGRN (ng/ml)
vehicle
5
50
OD (415nm)
3
2.5
2
1.5
1
0.5
0
*
PGRN (ng/ml)
vehicle
5
50

(E)

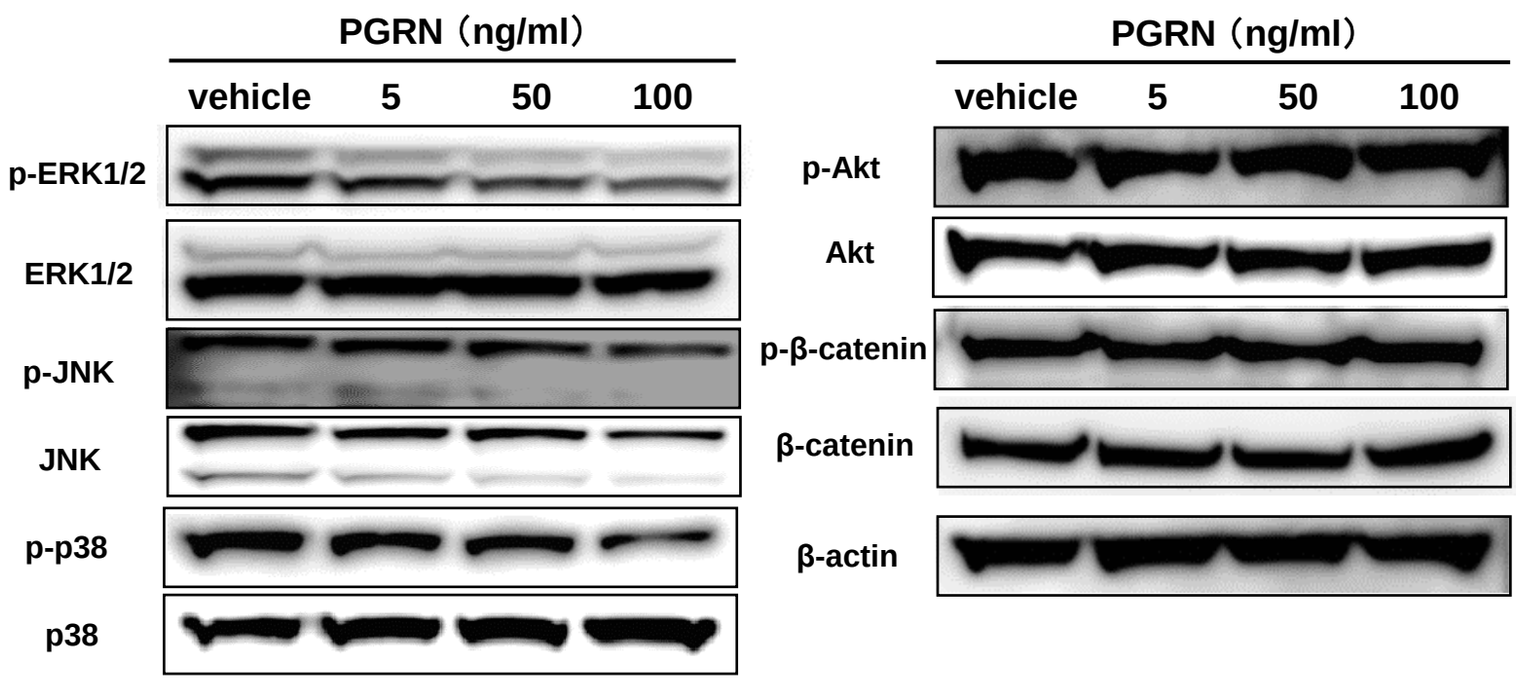
PGRN（ng/ml）
vehicle
5
50
100
p-ERK1/2
ERK1/2
p-JNK
JNK
p-p38
p38
PGRN（ng/ml）
vehicle
5
50
100
p-Akt
Akt
p-β-catenin
β-catenin
β-actin